A Uniform Sky Illumination Model to Enhance Shading of Terrain and Urban Areas

Patrick J. Kennelly
Department of Earth and Environmental Sciences
CW Post Campus of Long Island University
720 Northern Blvd.
Brookville, NY 11050 USA
(516) 299-2652
Patrick.Kennelly@liu.edu
Fax: (516) 299-3945
and

A. James Stewart
School of Computing
Queen's University
Kingston, Ontario, K7L 3N6 Canada
(613) 533-3156
jstewart@cs.queensu.ca

September 10, 2008

Abstract

Users of geographic information systems (GIS) usually render terrain using a point light source defined by an illumination vector. A terrain shaded from a single point provides good perceptual cues to surface orientation. This type of hill shading, however, does not include any visual cues to the relative height of surface elements.

We propose shading the terrain under uniform diffuse illumination, where light arrives equally from all directions of a theoretical sky surrounding the terrain. Surface elements at lower elevations tend to have more of the sky obscured from view and are thus shaded darker. This tinting approach has the advantage that it provides more detailed renderings than point source illumination.

We describe two techniques of computing terrain shading under uniform diffuse illumination. One technique uses a GIS–based hill shading and shadowing tool to combine many point source renderings into one approximating the terrain under uniform diffuse illumination. The second technique uses a C++ computer algorithm for computing the inclination to the horizon in all azimuth directions at all points of the terrain to map sky brightness to the rendering of the terrain.

To evaluate our techniques, we use two Digital Elevation Models (DEMs): the Schell Creek range of eastern Nevada and a portion of downtown Houston, Texas from Light Detection and Ranging (lidar) data. Renderings based on the uniform diffuse illumination model show more detailed changes in shading than renderings based on a point source illumination model.

Keywords: Illumination model, point source illumination, uniform diffuse illumination, shading, shadowing

1 Introduction

Illumination models are important in computer graphics to create realistic surface renderings. These models consist of a source of illuminating light and an illuminated surface, and can include atmospheric attenuation between the source and the surface, as well as ambient light distributed uniformly over the model (Foley et al. 1990).

Cartographers consider the same factors when shading terrain. Imhof (1982) discussed adding ambient light to uniformly brighten hill shading, and Thelin and Pike (1991) used ambient light in their shaded-relief map of the conterminous United States. The effects and use of atmospheric attenuation on rendering terrain are discussed by Brassel (1974), Imhof (1982), Ding and Desham (1994) and Patterson (2004).

The illuminated surface is also considered, especially the nature of the reflector. A matte surface reflects incident light in all directions equally and is called a diffuse reflector. A shiny surface reflects light most intensely in the direction that light is reflected off the surface and is called a specular reflector (Foley et al. 1990; Weibel and Heller 1991; Zhou 1992). Because most terrain elements behave more like a matte reflector, calculations for hill shading are usually based on such a reflector. Such surfaces are also said to obey Lambert's Law or be ideal Lambertian reflectors (Slocum et al. 2004).

The source of illuminating light has been the grounds of numerous discussions in cartographic literature. Researchers have discussed the appropriate direction of illumination vectors for rendering terrain, and the use of multiple illumination vectors, including ones that change the illumination source for a local portion of the terrain while keeping regional illumination constant. We summarize traditional thinking and current research on this subject below.

1.1 Direction of Point Source Illumination

The most commonly cited aspect direction for illuminating is from the northwest (Robinson et al. 1995). Imhof (1982) theorizes that this is because maps are generally oriented with north to the top, and users are accustomed to lighting from above and left, a legacy of our left to right writing, predominantly right-handed western culture.

Imhof (1982) also notes that northwest illumination had been an issue because this direction is not consistent with solar illumination in the northern hemisphere. The dilemma of illuminating from the south instead of north is that most map users perceive terrain ren-

dered with this lighting to be inverted (Imhof 1982; Robinson et al. 1995). Many aerial photographs and satellite images in the northern hemisphere show evidence of this terrain inversion effect. In practice, this artifact can be avoided in terrain rendering by using an aspect for illumination anywhere from the northern half of the sky. The aspect is often chosen at a right angle to the trend of elongate topographic features, or by trial and error for aesthetic considerations.

The vertical inclination angle from horizontal of a point illuminator is also important. Imhof (1982) suggests angles of less than 20^o for flat, undulating terrain and angles of 45^o or more for steep slopes. A low angle of illumination in high relief terrain will result in large areas being shadowed. Imhof (1982) dislikes shadows, as they are cast from some distance and have no relationship to the local terrain. In essence, shadowing can mask detailed areas of hill shading.

For digital terrain, shadows can be avoided in two manners. First, the user can select an angle at a large enough inclination to cast no shadows. This angle can be determined by calculating slope and identifying its maximum value. Second, the user can shade without shadowing. The calculation is identical for hill shading, and shadows are simply not computed. Although this is geometrically impossible, it is a quite common practice in relief mapping.

As the inclination angle approaches 90^o, the appearance of the rendering changes significantly. Imhof (1982) calls this slope shading, as brightness values with vertical illumination are identical to the cosine of the slope at each surface element. Slope shading follows the principle of "the steeper the darker" (Imhof 1982, page 162). For most users, the 3D effect is greatly diminished with vertical point source illumination.

1.2 Multiple Directions of Point Source Illumination

Local variations in direction of illumination were common before the advent of computer based terrain rendering. Imhof (1982) describes the aesthetic basis for such variations, and points out that they are especially effective at bringing out detail in ridges and valleys oriented parallel to the primary direction of illumination used for rendering. He suggests variations in the aspect and the inclination of the local illumination vector by angles of less than 30^o from the regional illumination vector. The resulting Swiss style shading is highly acclaimed for its detail and beauty. Brassel (1974) was the first to automate this technique, and Swiss cartographers continue to develop techniques in this fashion (Jenny and Raeber

2002).

An alternative methodology is to define multiple illumination vectors for the entire area, then devise a method to combine the renderings. The simplest way is to illuminate from different directions, then average the resulting hill shading and shadowing brightness values for the each surface elements (Hobbs 1995). The relative intensity of the illumination is easily included by multiplying by relative weights for each of the renderings from different illumination directions. A common example is the combination of northwestern, moderately inclined (30^o to 60^o) illumination with vertical illumination (Imhof 1982; Patterson and Hermann 2004).

Other lighting models begin with multiple illumination vectors at the regional level and use methods to combine renderings on a local level. Patterson (1997) suggests illuminating from different directions, visually comparing results, and using masks to select areas to include from each rendering. Mark (1992) suggests a more automated approach. He illuminates the island of Hawaii from four azimuths (225^o, 270^o, 315^o and 360^o) all with inclinations of 30^o. He then calculates the aspect of the terrain model, and applies weights for individual grid cells to each of the hill shaded grids, with larger differences between the illumination and aspect directions resulting in greater weighting. Mark's hill shading technique was also used by Schruben (1999) in his relief map of the conterminous United States.

Hobbs (1999) adds another variable to a multi-point model by illuminating from three different aspect directions using red, green and blue light sources. These illumination colors combine to render the terrain with a large range of colors. This technique combines regional variations in illumination direction with automated local variations in color to increase the visible detail of the rendering.

Although these techniques are quite varied, their commonality lies with researchers focusing on the surface to be illuminated and attempting to add more detail to specific locales than would be present in a rendering using one point source of illumination. We approach the challenge of offering additional detail to rendered surfaces from a different perspective. We explictly define a general illuninating source model that inherently adds more detailed shades of gray to any terrain surface.

1.3 Uniform Diffuse Illumination

A uniform diffuse illumination model assumes that the illuminating source of light is evenly distributed throughout a hemisphere at great distance, representing the sky. Rendering ter-

Point Source Illumination Uniform Diffuse Illumination

Figure 1: Overhead view of a ramp between two horizontal surfaces at different elevations. Uniform diffuse illumination provides perceptual cues to the relative elevations of the two surfaces, whereas hill shading does not (adapted from Stewart (2003)).

rain with this model adds details not present with renderings from a point source illumination model. While point source hill shading provides cues to the orientation of a surface, it does not provide visual cues to the relative elevation of the surface. One can infer elevation near sloping areas, since the bottom edge of a slope will be lower than the top edge. However, a conscious effort is necessary to make this inference. Furthermore, a degree of ambiguity remains, as shown in Figure 1.

Our goal is to shade the terrain in such a way as to provide more cues to relative surface elevation, particularly on terrain with large elevation differences, such as mountainous areas and urban areas with tall buildings. Our technique would work on any terrain, but areas with large variations in local relief also have large variations in the amount of ideal diffuse illumination received by nearby surface elements. Thus, variations in shading would be more subtle for relatively flat, featureless topography where a slightly inclined point source might reveal more detail of the topography.

In the remainder of the paper, we first describe the illumination model which defines how the terrain will be shaded. We then describe techniques of computing the terrain shading according to that model. Finally, we show example renderings of two digital elevation models: one of a mountainous region and one of an urban region.

2 The Illumination Model

The rendering equation (Kajiya 1986) completely describes the interaction of light with a surface. We will assume that the terrain is a Lambertian surface, which reflects light equally in all directions. For Lambertian surfaces, the rendering equation is

$$L_{out}(x) = \frac{\rho(x)}{\pi} \int_{H(x)} L(x, \omega) \ \cos(\gamma) \ d\omega$$

where (see Figure 2):

- $L_{out}(x)$ is the radiance emitted from surface point x. As a Lambertian surface, $L_{out}(x)$ is equal in all directions leaving x.
- $\rho(x)$ is the albedo at x.
- $L(x, \omega)$ is the radiance arriving at x from direction ω. Direction ω can be considered a vector, or a pair of (azimuth, inclination) angles.
- γ is the angle of direction ω with respect to the surface normal at x. $\cos(\gamma)$ is the parameter used in hill shading.
- $H(x)$ is the hemisphere of directions, ω, above the surface at x (i.e. those for which γ is at most 90 degrees)

Radiance is described in units of power per area per solid angle or, more specifically, Watts per square meter per steradian. However, the eye perceives "intensity" of radiance differently at different wavelengths. The Commission Internationale de l'Eclairage (CIE) standard photopic luminosity function (Gibson and Tyndall 1923) converts radiance, $L_{out}(x)$, to "luminance" which is proportional to perceived intensity. Luminance is measured in lumens per square meter per steradian. Our goal is to shade the terrain by computing an approximation of $L_{out}(x)$ at each point of the terrain.

The set, $H(x)$, of directions from which illumination arrives can be subdivided into two sets, those directions from the sky and those directions from the ground. Let $H(x) = S(x) \cup T(x)$, where $S(x)$ is the set of directions in which the sky is visible from x, and $T(x)$ is the set of directions in which another part of the terrain is visible from x. Then

$$L_{out}(x) \ = \ \frac{\rho(x)}{\pi} \int_{S(x)} L(x, \omega) \ \cos(\gamma) \ d\omega$$

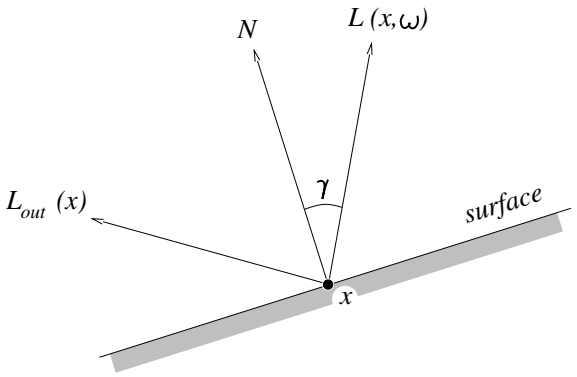

Figure 2: The outgoing radiance, $L_{out}(x)$, depends upon the incoming radiance, $L(x, \omega)$, from each direction, ω, in the visible sky above the surface. N is the surface normal. $L_{out}(x)$ has no directional variation, since the surface is Lambertian.

$$+ \frac{\rho(x)}{\pi} \int_{T(x)} L(x, \omega) \ \cos(\gamma) \ d\omega$$

This expresion for $L_{out}(x)$ can be simplified by approximating the radiance arriving at x from other points on the terrain. A first–order approximation of $L_{out}(x)$ ignores radiance arriving from other terrain points, assuming that $L(x, \omega)$ is zero for directions ω in T. A slightly better approximation (Stewart and Langer 1997) assumes that $L(x, \omega) = L_{out}(x)$ for directions ω in T. This approximation is motivated by the rough observation that (bright) points on peaks get light from other bright points on peaks, and (dark) points in valleys get light from other dark points in valleys.

In this paper, we will use the first–order approximation, which we will call "direct primary illumination" since it considers only direct illumination from the sky. We will also assume that incoming illumination from a direction ω is the same at all points on the terrain: $L(x, \omega) = L(\omega)$. From the second assumption, it follows that the sky is very distant from the terrain, or that the terrain is very small with respect to the sky.

$$L_{out}(x) \approx \frac{\rho(x)}{\pi} \int_{S(x)} L(\omega) \ \cos(\gamma) \ d\omega \tag{1}$$

To evaluate Equation 1 at a terrain point, x, we need

- the albedo, $\rho(x)$,
- a description of the sky, $S(x)$, visible from x, and
- values for $L(\omega)$ from all sky directions.

Note that, in general, $S(x)$ varies with x, since different parts of the sky are visible from different points on the terrain, and that $L(\omega)$ varies with ω, since the sky is usually not of uniform intensity. At a point, p, on a peak, $S(p)$ would consist of the entire sky while at a point, v, in a valley, $S(v)$ would be reduced by the valley walls.

The next sections describe how $L(\omega)$ can model common patterns of sky illumination.

2.1 Single and Multiple Point Illumination

A "single point" of light doesn't exist in nature. A single point would subtend a solid angle of zero as seen from any point on the terrain, and would thus make no contribution to the integral of Equation 1.

Instead, a point source can be modelled as a very bright spot in the sky, the intensity of which drops quickly with increasing distance from the center of the spot. This dropoff can be modelled, for example, as $\cos^n(\gamma)$, where γ is the angular deviation from the center of the spot, and n is any integer (typically between 10 and 400).

For a point source with center in direction ω_c, the radiance can be modelled as:

$$L(\omega) = \begin{cases} 0 & \text{if the dot product } \omega \cdot \omega_c \text{ is negative} \\ L_{max}\ (\omega \cdot \omega_c)^n & \text{otherwise} \end{cases}$$

where L_{max} is the (maximum) radiance at the center of the spot. See Figure 3.

Sharp single point illumination provides cast shadows and shading based on orientation of slope and aspect, but does not provide the cues to relative surface elevation that we get with uniform diffuse illumination.

Multiple point sources can be modelled defining $L(\omega)$ as the sum of the contributions from several point sources. Different colors of multiple point sources can be modelled by making $L(\omega)$ a function of wavelength, or by making it a red–green–blue tuple (e.g. Hobbs 1999).

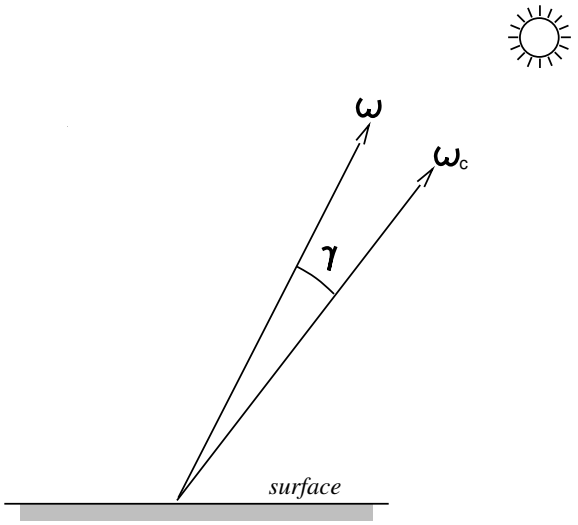

Figure 3: The radiance of a point light source can be modelled as $\cos^n(\gamma)$, where γ is the angle between the light source direction, ω_c, and the viewing direction, ω.

2.2 Uniform Diffuse Illumination

Our model of sky illumination has equal radiance arriving from all directions in the sky:

$$L(\omega) = L$$

where L is a constant radiance.

With such uniform diffuse illumination, the radiance of a terrain point is determined primarily by how much of the sky is visible from the point. Surfaces in valleys are darker because less of the sky is visible from these locales.

The radiance of a terrain element is also determined by its orientation with respect to the direction of illumination, due to the cosine term in Equation 1. Uniform diffuse illumination produces detailed renderings similar to those made with point source illumination, but also accounts for the distribution of illumination throughout the sky.

3 Techniques of Computation

The preceding section described the local reflectance model (Equation 1) and a sky model, $L(\omega)$. We will now discuss two techniques to compute terrain shading from these models.

3.1 A GIS–Based Technique

Our first technique of shading the terrain relies on the tools available in a standard GIS. This technique approaches the problem in the traditional manner: from the sky to the surface. We determine which grid cells are visible from selected directions in the sky.

With the GIS, we can create a shaded and shadowed grid for any selected direction of point source illumination. We will borrow an approach from the field of computer graphics and will model the sky illumination, $L(\omega)$, as a set of point sources scattered across the sky (e.g. Watt 1999). By summing weighted contributions from all the scattered point sources, we achieve an approximation of the uniform diffuse illumination, which provides more cues to relative surface elevation.

We represent the sky as a hemisphere, and a point source in a particular direction as a point on the hemisphere. The point sources are distributed upon the hemisphere at regular intervals of aspect and inclination. Figure 4 shows a regular distribution of point sources at 15^o spacing in both azimuth and inclination.

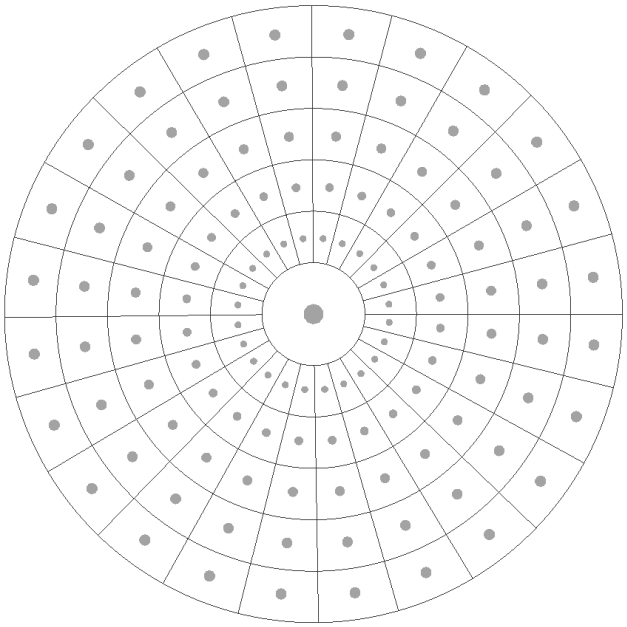

Figure 4: Point light sources distributed with 15^o spacing in azimuth and inclination. The center of the circle corresponds to an inclination of 90^o, and the circumference to an inclination of 0^o. Each point light source approximates the illumination from the area of sky around it, shown by the divisions of the hemisphere. The area of each sector is proportional to the weight of the corresponding point source. In the figure, the area of each dot is in proportion to the weight of the source.

Let G_i be the grid that is shaded and shadowed by the i^{th} point source. Then the final grid computed as

$$G = \sum_i w_i \, G_i$$

where w_i is the weight that we assign to the i^{th} point source.

To determine the weights of the point sources, consider that each point source, p_i, is representing the illumination from a small region of sky around p_i. Figure 4 shows these regions. All of the point sources are together representing the total illumination of the sky.

Let R_i be the area on a hemisphere of radius one which corresponds to the sky around p_i. Under the uniform sky model, light arrives equally from all directions in the sky, so the total light arriving from p_i is proportional to the area of R_i. In other words, the weight of p_i should be proportional to the area of R_i. Since the total surface area of the unit hemisphere is 2π, we will define

$$w_i = \frac{1}{2\pi} \, R_i$$

so that the sum of the weights is equal to one.

If we distribute the point sources every a radians in azimuth and every e radians in inclination, then each point source, p_i, represents an area of sky which is a radians wide and e radians high, centered at p_i. If p_i is located at inclination θ and azimuth ϕ, the size of the area surrounding p_i is

$$\begin{aligned} R(\theta, \phi) &= \int_{\theta - e/2}^{\theta + e/2} \int_{\phi - a/2}^{\phi + a/2} \cos(\theta) \; d\phi \; d\theta \\ &= a \; (\sin(\theta + e/2) - \sin(\theta - e/2)) \end{aligned}$$

The weight of a sample point at inclination θ is thus

$$w(\theta) = \frac{a}{2\pi} \; (\sin(\theta + e/2) - \sin(\theta - e/2)). \tag{2}$$

In addition to the point sources spaced evenly in azimuth and inclination, we add a single point source at the zenith. This single zenith source replaces a ring of $\frac{2\pi}{a}$ point sources which would otherwise be clustered tightly around the zenith, each having very small weight. The zenith source is used simply to reduce the number of sources, in order to make the computation more efficient.

The zenith source corresponds to the portion of a hemisphere sliced by a plane perpendicular to the hemisphere's radius centered at the zenith and subtending an angle of e radians.

The area of this portion of the hemisphere is

$$\begin{aligned} R_{zenith} &= \int_{\pi/2-e}^{\pi/2} \int_{0}^{2\pi} \cos(\theta)\ d\phi\ d\theta \\ &= 2\pi\ (1 - \cos e) \end{aligned}$$

and its weight is thus

$$w_{zenith} = 1 - \cos e.$$

Given all of the $N = \frac{2\pi}{a}(\frac{\pi}{2e} - 1) + 1$ point sources, we use the GIS to render the grid under each point source, separately. The N grids cells are weighted according to the corresponding point source weights and summed to produce a grid that is shaded and shadowed under uniform diffuse illumination. Note that the GIS rendering automatically accounts for the cosine term in Equation 1.

3.2 The Horizon Technique

Our second technique of shading the terrain takes a different approach. Rather than determining which parts of the terrain are shadowed from points in the sky, we determine which parts of the sky are visible from points on the terrain. In essence, we compute the horizon for all directions of azimuth at every point on the terrain.

For each grid cell, x, a visibility analysis determines the horizon in all azimuth directions from x. The horizon data are stored with each grid cell, and define the boundary of the sky that is visible from the grid cell. The horizon at a cell, x, thus defines the visible sky, $S(x)$, which can be used in Equation 1 to calculate the shading of cell x.

The horizon at a point, x, is the boundary between the terrain and the sky, as seen from x. The horizon inclination, Θ, can be represented as a function of azimuth angle, ϕ:

$$\Theta(x, \phi).$$

We measure inclination as zero at the horizontal, increasing upward to 90 degrees at the zenith.

For the purpose of computing direct primary illumination, it is sufficient to use an approximation of the actual horizon. The approximation divides the azimuthal directions into a number of "sectors." In each sector, the horizon inclination is approximated with a single inclination angle which can be either the maximum or the average horizon inclination within

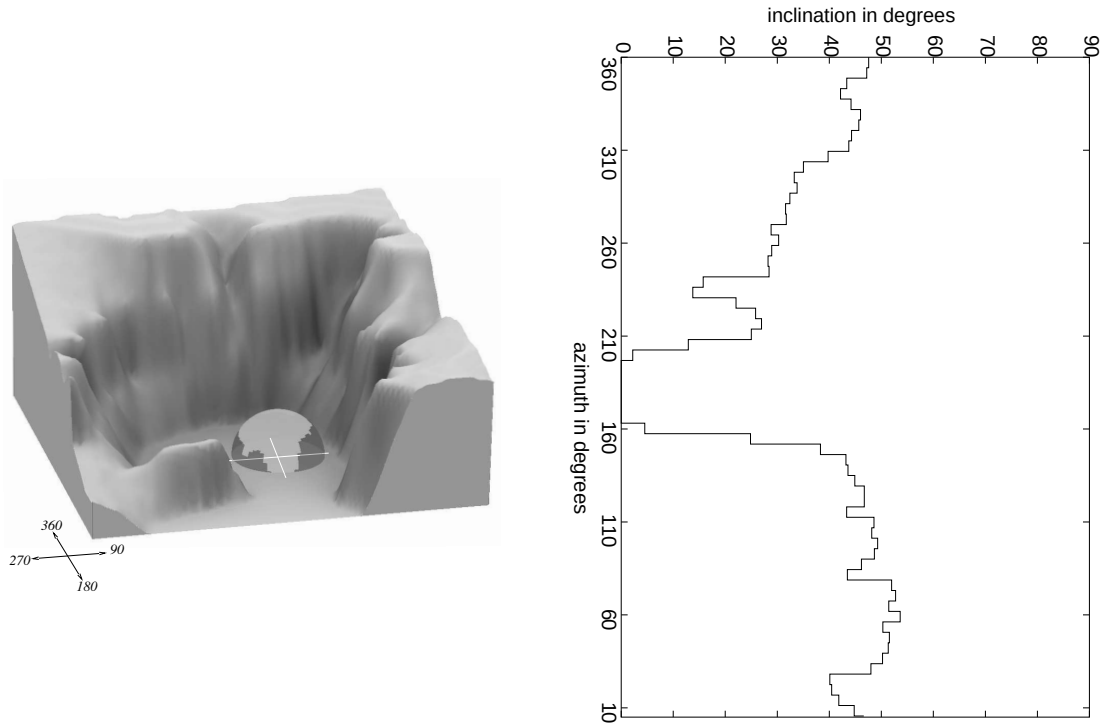

Terrain with Point

Approximate Horizon

Figure 5: The approximate horizon is shown (right) for a point on a terrain (left). The point is shown surrounded by a hemisphere on which the approximate horizion is shown in dark gray.

that sector. The approximate horizon is a piecewise-constant function of aziumth angle. Let $\Theta_i(x)$ be the horizon inclination in the i^{th} sector surrounding x. Figure 5 shows a point on a terrain, and the approximate horizon at the point.

3.2.1 Algorithms to Compute the Horizon

Several algorithms are available to compute the approximate horizon at each grid cell. An approach by Max (1988) sampled the horizon in eight sectors around each point of a gridded terrain, and illuminated the point in proportion to the fraction of the sun's disc that appeared above the horizon. Cabral et al. (1987) used 24 sampling directions around each point of a triangulated terrain. Stewart (1997) described a computer algorithm for efficiently computing the horizon at all terrain points, of any number of sectors. For large terrains, this algorithm performs substantially faster than other approaches. Stewart's algorithm takes

about 10 minutes on a 1 GHz PC to compute the horizons of a 500 by 500 grid.

3.2.2 Calculation of Terrain Radiance from Horizons

Given a horizon, $\Theta(x, \phi)$, at each terrain cell, x, we now calculate the radiance, $L_{out}(x)$. From Equation 1, we integrate the incoming radiance over the visible sky, $S(x)$:

$$L_{out}(x) \approx \frac{\rho(x)}{\pi} \int_{S(x)} L(\omega)\ \cos(\gamma)\ d\omega$$

The domain of integration, $S(x)$, can be mapped onto azimuth, ϕ, and inclination, θ, by replacing the infinitesimal solid angle, $d\omega$, with the corresponding infinitesimal surface element on the unit sphere, $\cos(\theta)\ d\phi\ d\theta$ (recall that inclinations, θ, are measured upward from the horizontal):

$$L_{out}(x) \approx \frac{\rho(x)}{\pi} \int_0^{2\pi} \int_{\Theta(x,\phi)}^{\pi/2} L(\theta, \phi)\ \cos(\gamma)\ \cos(\theta)\ d\theta\ d\phi$$

First, the inner integral is removed. We take advantage of our illumination model in which $L(\theta, \phi) = L$ is constant, and use the MAPLE symbolic mathematics package (`www.maplesoft.com`) to simplify the expression. The MAPLE package reduces the above equation to

$$L_{out}(x) \approx \frac{\rho(x)}{2\pi} \int_0^{2\pi} \cos\epsilon\ \left(\frac{\pi}{2}\ \sin\delta - s\cos\delta\cos^2\Theta - \sin\delta\sin\Theta\cos\Theta - \Theta\ \sin\delta\right)\ d\phi$$

where: $\Theta = \Theta(x, \phi)$; δ is the angle between the surface normal and the vertical direction; ϵ is the angle between azimuth angle ϕ and the projection of the surface normal onto the horizontal plane; and s is equal to $+1$ if the the projection of the surface normal onto the horizontal plane is in the same direction as ϕ, and equal to -1 otherwise.

Next, the outer integral is removed. Given an approximate horizon, $\Theta_i(x)$, which is constant across each sector, i, we can sum over the sectors rather than integrate over the aziumth angles:

$$L_{out}(x) \approx \frac{\rho(x)}{2\pi} \sum_{i=0}^{N_s-1} \frac{2\pi}{N_s} \cos\epsilon\ \left(\frac{\pi}{2}\ \sin\delta - s\cos\delta\cos^2\Theta_i - \sin\delta\sin\Theta_i\cos\Theta_i - \Theta_i\ \sin\delta\right)$$

where N_s is the number of sectors and ϕ_i is the aziumth angle at the middle of sector i ($\phi_i = (i + 0.5)(2\pi/N_s)$).

The above expression shades the terrain by incorporating the albedo, the orientation of the surface normal vector with respect to the illumination vector, the sky model, and the

horizons. Given the horizons computed by an algorithm from Section 3.2.1, the expression can be evaluated very quickly. A terrain of 500x500 cells can be shaded in less than one second on a 1Ghz PC (after the initial compution of the horizons).

4 Rendered Elevation Models

We use the uniform diffuse illumination model to render digital elevation models (DEMs) of a mountainous area and an urban setting. Both of these models show significant differences between renderings with a point source of illumination and diffuse sky illumination.

We render a one arc second DEM of a portion of the Schell Creek range of eastern Nevada. We use this model because the range has valleys of various width and orientation. Because variable portions of the sky are visible from different sites within these valleys, the diffuse illumination model should reflect this variability. The grid is approximately 1084 by 1690 grid cells and has 28 meter resolution. We use a vertical exaggeration of five times to highlight shadows. Elevation data and the associated slope map are shown in Figure 6(a) and Figure 6(b), where higher elevations and flatter slopes are brighter.

We use lidar data from an urban area to illustrate the extra detail and cues to relative surface elevation that are provided with uniform diffuse illumination. Such data often result in renderings that have numerous flat areas including streets and the tops of buildings, which are not well differentiated with normal point source illumination, and which have numerous shadows that mask other information. Elevation data of this area are shown in Figure 6(c) and Figure 6(d).

We wish to compare the uniform diffuse illumination of the Schell Creek range with the best possible rendering under classical point source conditions. We will consider point source rendering with and without shadows, using an illumination vector from an azimuth of 45^o and an inclination of 45^o. To create the diffuse rendering, we will use the GIS Technique with 121 point samples spaced 15^o apart (see Figure 4).

Under illumination by a single point source (Figure 7(c)), the terrain rendering resembles typical hill shaded maps of mountainous areas. Areas of intermediate slope and with aspects facing towards the direction of illumination are brightest, and areas of steep slope and with aspects facing away from the direction of illumination are darkest. Flat areas are shaded with an intermediate gray.

If shadows are added to the point source illumination (Figure 7(d)), terrain elements

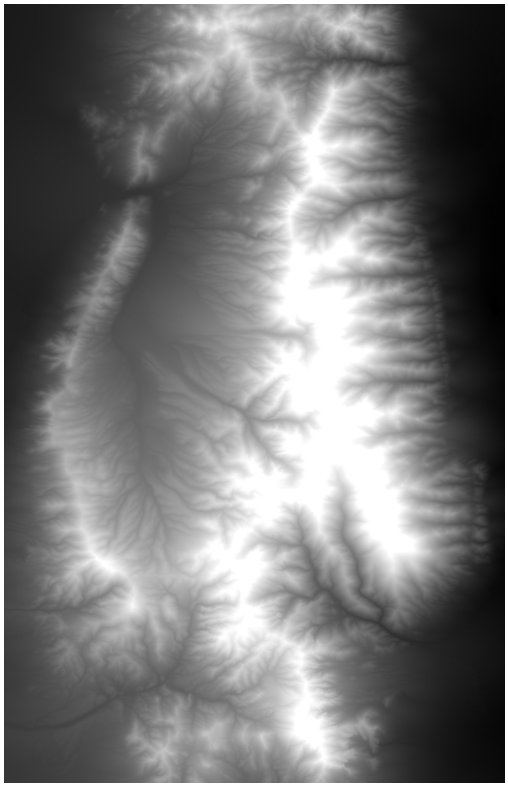

(a) Terrain hypsometric shading

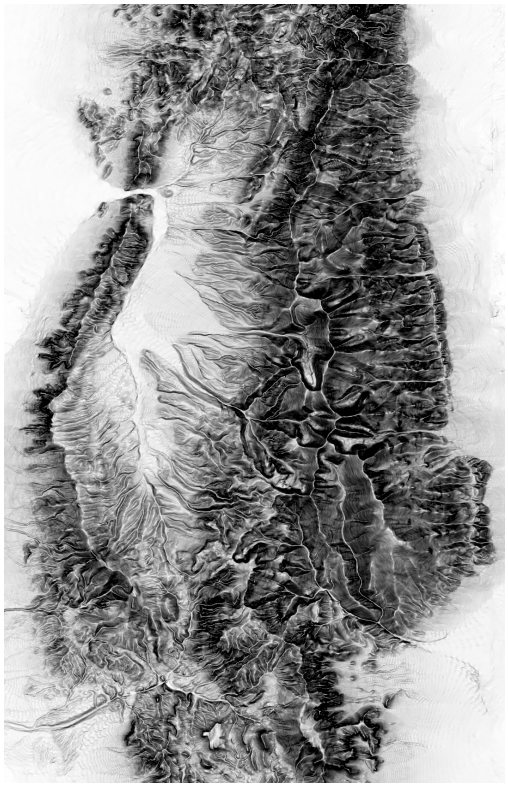

(b) Terrain slope shading

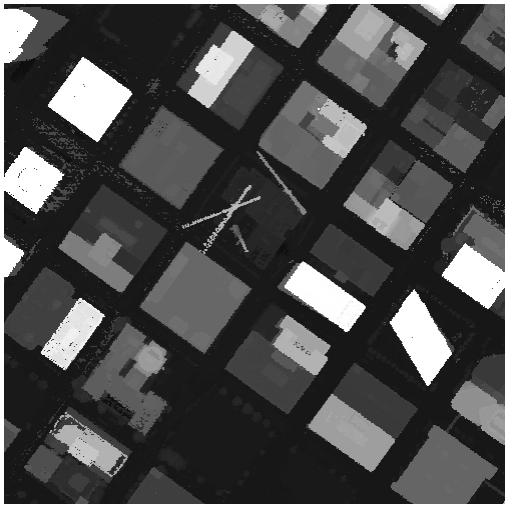

(c) Urban hypsometric shading

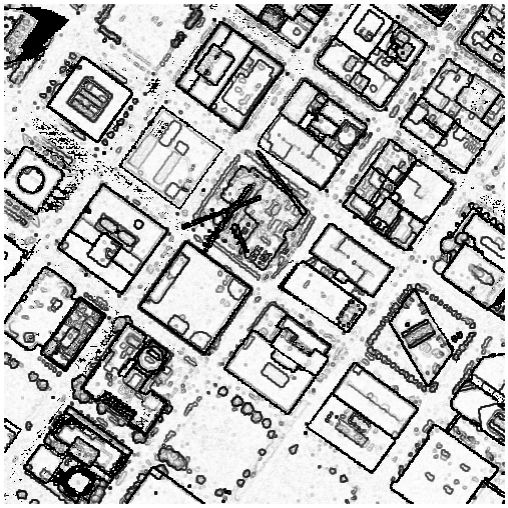

(d) Urban slope shading

Figure 6: Two data sets were used to evaluate the diffuse illumination method: The Schell Creek range of eastern Nevada provides a typical variety of elevations (between 1691m and 3627m); and part of downtown Houston, Texas provides extreme elevation changes (between 13m and 408m, with the highest elevation due to, we believe, a radio mast).

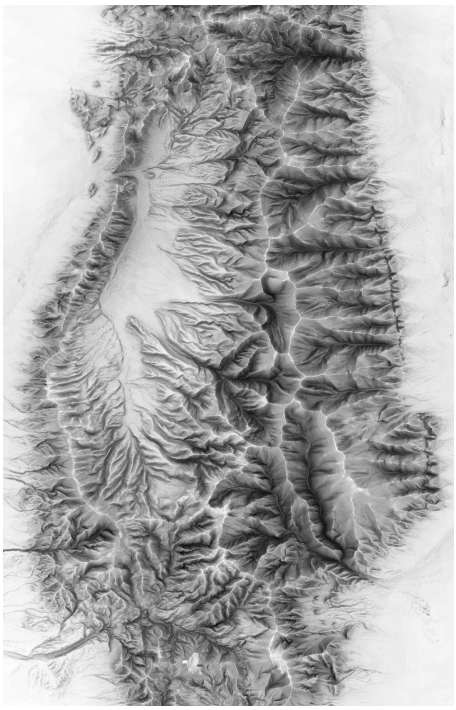

(a) Diffuse illumination

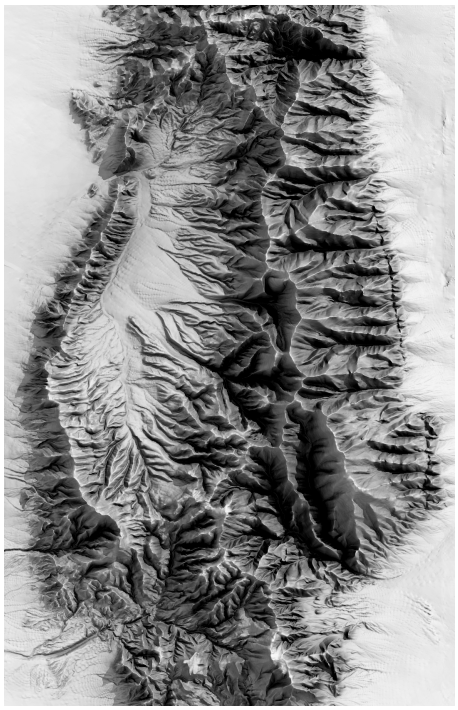

(b) Diffuse illumination with shadows

(c) Point illumination

(d) Point illumination with shadows

Figure 7: The different illumination methods applied to the Schell Creek range (vertically exaggerated by a factor of five).

that occur in this shadowed area are assigned a darker color. In those areas, the values are reduced by 20%. Because we use a northeast light source, shadows occur to the south and west of ridges. Areas outside of the shadows are unaffected, and have the same brightness values as in Figure 7(c).

Diffuse illumination shades this topography in a much different manner (Figure 7(a)). The rendering is different from the point source illumination (Figures 7(c) and 7(d)) and from hypsometric shading (Figure 6(a)) or shading based on slopes (Figure 6(b)). Hypsometric tinting can be described as "the lower, the darker," and slope shading can be described as "the steeper, the darker." The rendering shown in Figure 7(a), however, can be described as "the less visible sky, the darker."

Examination of Figure 7(a) shows that ridges are very bright features, as most or all of the sky will generally be visible. Flat areas away from the range are also bright, as little of the sky is obscured by topography. A wide valley, such as the north–south trending valley within the northwestern portion of the range, will also be relatively bright for the same reason. Narrow, more obscured valleys, however, are darker. A good example is the north–south trending valley between two ridges in the east–central portion of the map. This valley also shows other subtleties of the technique. It gets progressively darker at lower elevations, as less of the sky is visible. In the center of the valley, however, the valley bottom is flat and the cosine term of Equation 1 provides slightly increased brightness. This effect is visible in most valleys and rivers, and provides a cue to a local elevation minimum.

The diffuse illumination model represents equal brightness from all segments of the sky. As such, no shadows from any particular point source of illumination are apparent. Shadows from a point illumination source, however, can add important visual clues to the relative elevation of elevation models. We present Figure 7(b), a combination of renderings from diffuse illumination and point shadowing using weights of four and one respectively, for visual comparison with Figure 7(d), a combination of renderings from point hill shading and point shadowing in the same ratio.

To further illustrate our technique, we look at data from an urban elevation model. The frequent, rapid and extreme changes in elevation create a landscape well suited to rendering with diffuse illumination. We use a DEM of a portion of downtown Houston derived from lidar data. The 500 by 500 grid is at one meter resolution. Because of the inherently large relief of the elevation model, we do not use vertical exaggeration.

Under illumination by a single point source (Figure 8(c)), all flat areas are shaded with the

same color, making it very difficult to discern height differences. Uniform diffuse illumination (Figure 8(a)) darkens areas where less light arrives, providing strong cues to the relative elevations of the flat surfaces.

More detail under point source illumination is provided by combining a hill shaded rendering with a shadowed rendering, as shown in Figure 8(d), which has a point illumination source at an azimuth of 45^o and an inclination of 50^o from horizontal. But terrain features *within* the shadows do not themselves cast shadows, so only the highest features are provided with effective elevation cues. The combination of uniform diffuse illumination with shadowed rendering (Figure 8(b)) provides more elevation cues.

4.1 Renderings with the GIS-Based Technique

The urban renderings under uniform diffuse illumination were made with the Horizon Technique, described in Section 3.2. The Horizon Technique is very accurate and provides a benchmark to which other rendering techniques can be compared. It cannot be easily implemented using traditional GIS tools such as viewshed analysis tools, which can define intervisibility between locales on the same surface, but not intervisibility between locales on one surface (the terrain) and areas on another surface (the hemisphere representing the sky).

The GIS sky–to–surface technique described in Section 3.1 is instead used to define shading and shadowing from multiple sectors of the sky. The result is a discretized approximation of ideal diffuse illumination. Renderings with an insufficient number of sample points will contain shadow and shading artifacts. We varied the number of sample points to visually inspect such artifacts, comparing results with those of the Horizon Technique. We used points distributed in even increments of azimuth and inclination, as described in Table 1. The points were weighted according to Equation 2, as shown in Figure 9

Figure 10 shows the renderings using the GIS Technique with different numbers of sample points. We observe that 121 points are necessary to remove most shadow artifacts, and 529 points are necessary for smooth shading of flat surfaces. Figure 11 shows the larger urban area rendered with 121 and 529 sample points for comparison with Figure 8(a).

5 Discussion

Other researchers in terrain rendering and terrain parameterization have looked at mapping the visible sky as a hemisphere. They have looked at the inclination at which the surrounding

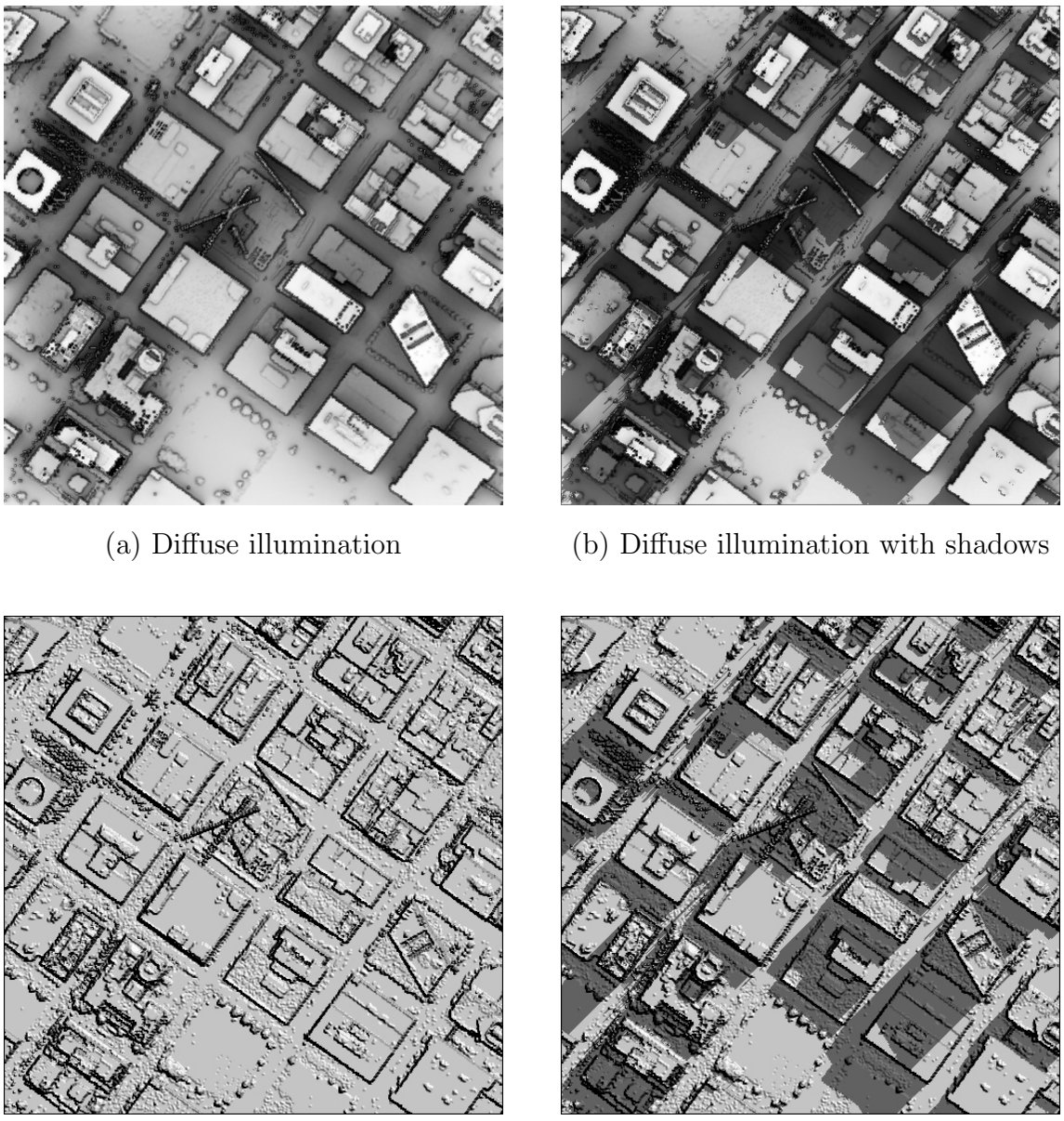

(a) Diffuse illumination

(b) Diffuse illumination with shadows

(c) Point illumination

(d) Point illumination with shadows

Figure 8: The different illumination methods applied to the Houston data.

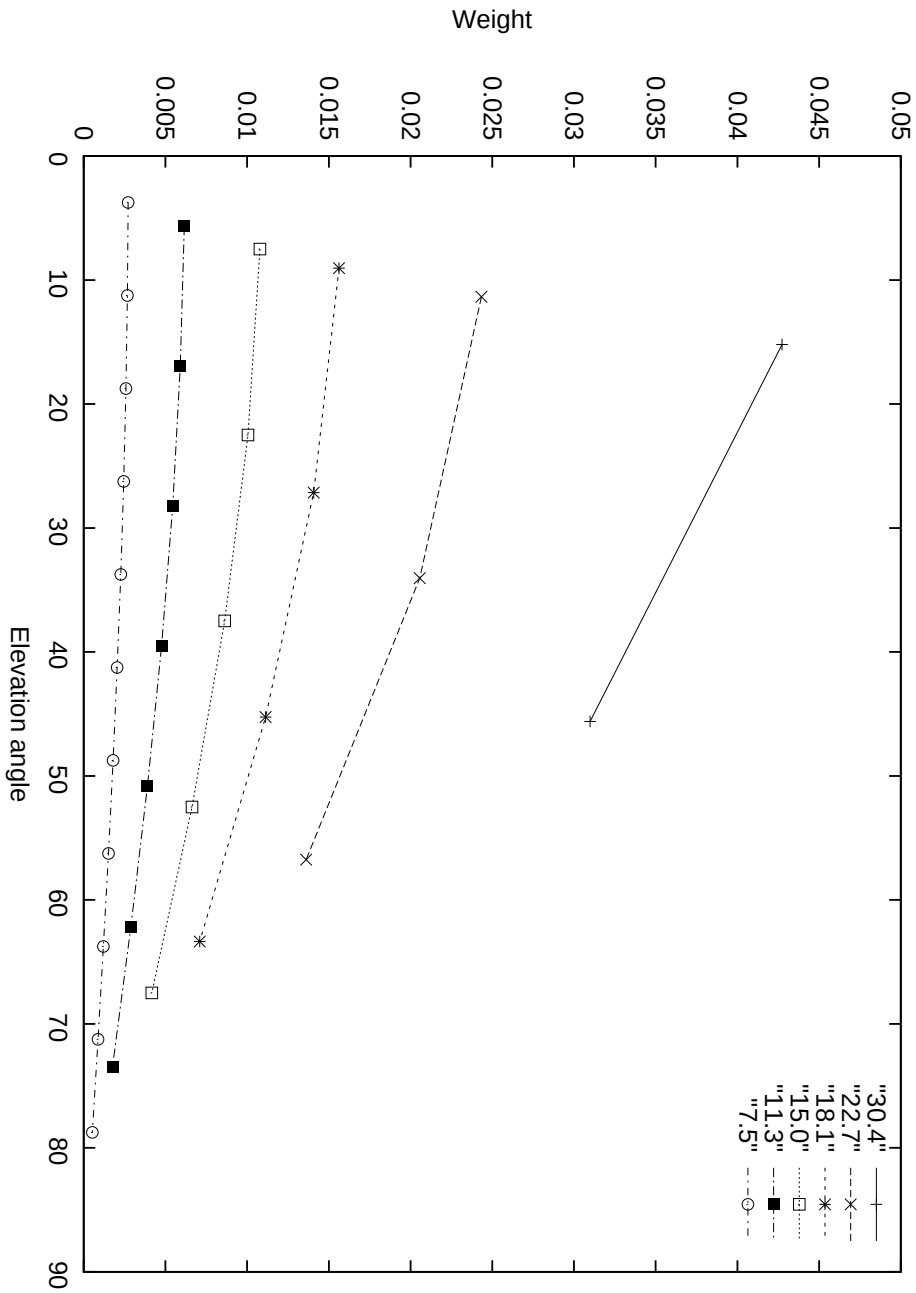

Figure 9: The weights given to sample points at various elevations are shown for different inclination spacings (30.4^o, 22.7^o, 18.1^o, 15.0^o, 11.3^o, and 7.5^o), calculated according to Equation 2. The weight of the larger sample at the pole is not shown, as it is very much larger than the other weights.

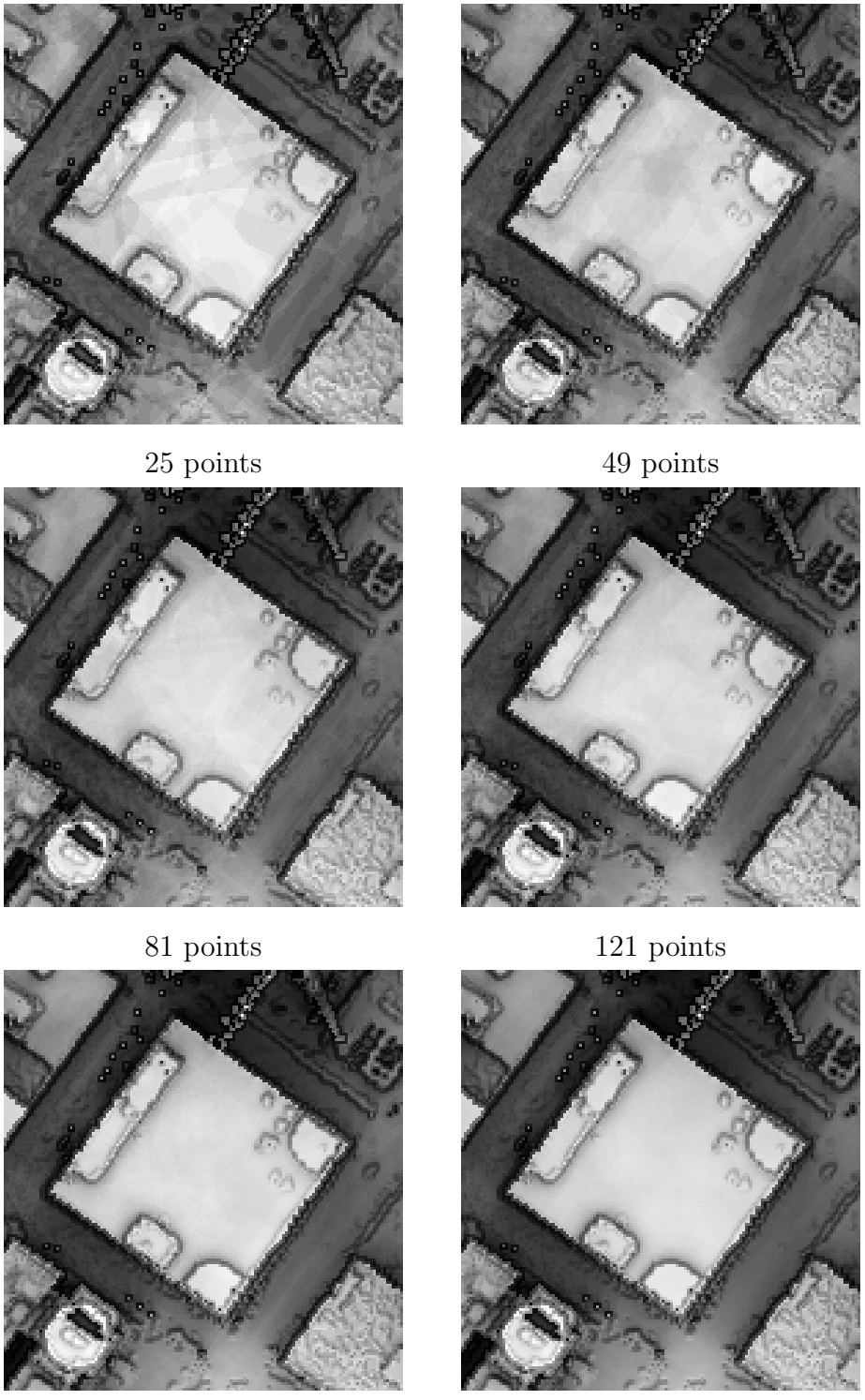

Figure 10: Uniform diffuse illumination of the Houston data, calculated using the GIS Technique with 25 to 529 sample points. Shadow artifacts are still visible with 121 sample points and are completely eliminated with 529 sample points.

Table 1: Distribution of sample points for various numbers of sample points using the GIS Technique.

Number of points	Azimuth separation	Inclination separation
25	30.4^o	30.4^o
49	22.7^o	22.7^o
81	18.1^o	18.1^o
121	15.0^o	15.0^o
225	11.3^o	11.3^o
529	7.5^o	7.5^o

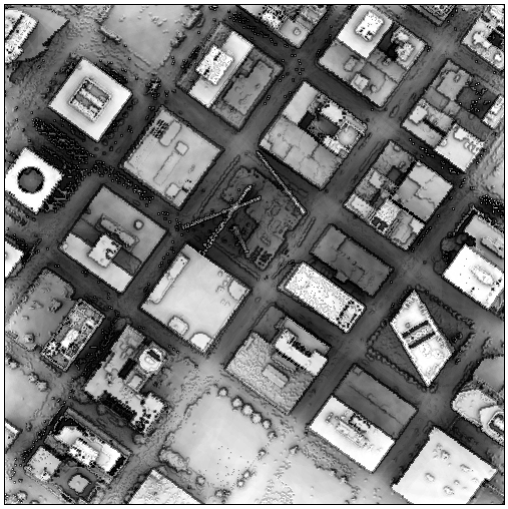

121 sample points

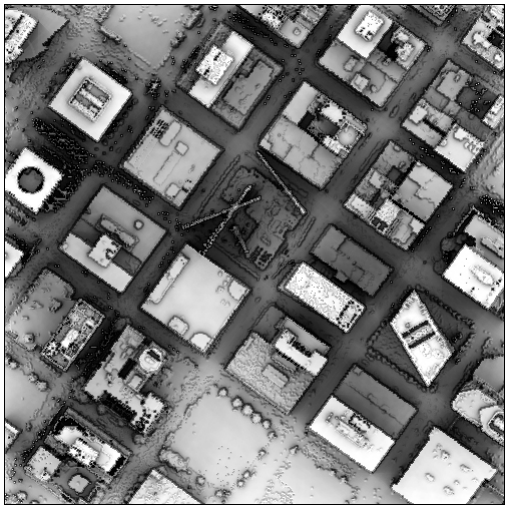

529 sample points

Figure 11: The 500×500 terrain, rendered with the GIS Technique using 121 and 529 sample points.

terrain will block visibility of the sky for a number of azimuth directions, but then calculated an average of these angles of inclination. This average angle is used to approximate diffuse illumination of the surface.

Yokoyama et al. (2002) define a terrain parameter called "openness" which expresses the degree of dominance or enclosure of a surface location. They use a line–of–sight algorithm along eight azimuth directions, and find the average of the associated zenith angles. They use these results to apply shades of gray to a map of terrain. They note details and contrasts on this image that are not apparent from elevation, slope, or hill shaded maps.

Corripio (2003) calculates the percentage of visible sky, or sky view factor, by looking at the ratio of area of the entire hemisphere projected vertically onto a plane versus the area of the visible sky defined by its average angle to the virtual horizon projected vertically onto a plane. Corripio uses 15^o samples of azimuth, and 1^o samples of inclination from horizontal to 45^o, which would find all virtual horizons in areas with slopes less than 45^o.

Averaging the angle of inclination in various aspect directions is a simplification that we do not make in our techniques. Corripio (2003) recognizes this simplifying assumption, and suggests storing azimuth and associated inclination information for refinement. With the Horizon Technique, these additional data are stored for each surface element, and with the GIS Technique they are stored in separate grids rendered for each point source illumination.

Fu and Rich (1999, 2002) designed and implemented software in a GIS environment to model solar radiation (insolation) based on topography. They explicitly model the horizon using a discretization of azimuth and inclination angles. Their application accounts for atmospheric conditions, elevation, surface orientation, and influences of surrounding topography using a surface to sky approach. Their methodology is similar in approach to the Horizon Technique described in this paper. They do not use their application to shade topographic surfaces. Instead, they look at a number of environmental applications, including physical and biological processes in agriculture and forestry, which are affected by the degree of insolation.

6 Summary

Classical point source shading provides cues to orientation of surface features by shading. Additionally, cast shadows from one direction of illumination provide cues to the relative elevation of proximate surface elements. Uniform diffuse illumination simply sums shading

and shadowing information from all portions of an evenly illuminated sky to provide a rendering with additional detail. The brightness of a surface under ideal diffuse illumination is a function of the amount of the visible sky.

We describe two techniques for rendering surfaces with uniform diffuse illumination. The first uses hill shading and shadowing tools common to GIS, and sums rendered grids from multiple, evenly spaced point illumination sources throughout the sky. The second more detailed technique defines a horizon in all directions of azimuth for each surface element. As the second approach is a more exact solution, we use this as a benchmark to compare our results with varying number of point sources for the GIS Technique. We found that most shadow artifacts are removed with 121 points and that flat surfaces are smoothly shaded with 529 points.

7 Acknowledgements

We would like to thank Dr. Anju Ding, Lead Applications Developer for TerraPoint, LLC for providing the lidar data of Houston, Texas. We would also like to thank CaGIS editor Lynn Usery and the anonymous reviewers for their many helpful suggestions. The terrain data was part of the National Elevation Dataset DEM from the U.S. Geological Survey National Map Seamless Distribution System website at seamless.usgs.gov.

References

Brassel, K. (1974). A model for automatic hill–shading. *The American Cartographer 1*(1), 15–27.

Cabral, B., N. Max, and R. Springmeyer (1987). Bidirectional reflection functions from surface bump maps. *Computer Graphics 21*, 273–281.

Corripio, J. (2003). Vectorial algebra algorithms for calculating terrain parameters from DEMs and solar radiation modeling in mountain terrain. *International Journal of Geographic Information Science 17*(1), 1–23.

Ding, Y. and P. Densham (1994). A loosely synchronous, parallel algorithm for hill shading digital elevation models. *Cartography and Geographic Information Systems 21*(1), 5–14.

Foley, J. D., A. van Dam, S. K. Feiner, and J. F. Hughes (1990). *Computer Graphics: Principles and Practice*. Reading, MA: Addison–Wesley.

Fu., P. and P. Rich (1999). Design and implementation of the Solar Analyst: an ArcView extension for modeling solar radiation at landscape scales. In *19th Annual ESRI User Conference*. http://gis.esri.com/library/userconf/proc99/proceed/papers/pap867/p867.htm.

Fu., P. and P. Rich (2002). A geometric solar radiation model with applications in agriculture and forestry. *Computers and Electronics in Agriculture 37*, 25–35.

Gibson, K. and E. Tyndall (1923). Visibility of radiant energy. In *Scientific Papers of the Bureau of Standards*, Volume 19, pp. 131–191.

Hobbs, F. (1995). The rendering of relief images from digital contour data. *The Cartographic Journal 32*(2), 111–116.

Hobbs, F. (1999). An investigaton of RGB multi–band shading for relief visualisation. *The International Journal of Applied Earth Observation and Geoinformation 1*(3–4), 181–186.

Imhof, E. (1982). *Cartographic Relief Presentation*. Berlin and New York: Walter de Gruyter.

Jenny, B. and S. Raeber (2002). Production of shaded relief with digital tools. In *International Cartographic Association – Mountain Cartography Workshop Proceedings*. http://www.karto.ethz.ch/ica-cmc/mt_hood/proceedings.html.

Kajiya, J. (1986). The rendering equation. *Computer Graphics 20*(4), 143–150.

Mark, R. (1992). Multidirectional oblique–weighted shaded relief image of the island of hawaii. Technical Report OF92–422, US Geological Survey Open File Report.

Max, N. (1988). Horizon mapping: Shadows for bump–mapped surfaces. *The Visual Computer 4*(2), 109–117.

Patterson, T. (1997). A desktop approach to shaded relief production. *Cartographic Perspectives 28*, 38–40.

Patterson, T. (2004, April). Creating Swiss–style shaded relief in Photoshop. http://www.shadedrelief.com/shading/Swiss.html.

Patterson, T. and M. Hermann (2004, April). Creating value–enhanced shaded relief in Photoshop. http://www.shadedrelief.com/value/value.html.

Robinson, A., J. Morrison, P. Muehrcke, A. Kimerling, and S. Guptill (1995). *Elements of Cartography, 6th ed.* New York: John Wiley and Sons.

Schruben, P. (1999). Color shaded relief map of the conterminous United States. Technical Report OF99–011 (Map with accompanying text), US Geological Survey Open File Report.

Slocum, T., R. McMaster, F. Kessler, and H. Howard (2004). *Thematic Cartography and Geographic Visualization, 2nd Edition*. Upper Saddle River, NJ: Pearson Prentice–Hall, Inc.

Stewart, A. (1997). Fast horizon computation at all points of a terrain with visibility and shading applications. *IEEE Transactions on Visualization and Computer Graphics 4*(1), 82–93.

Stewart, A. (2003, October). Vicinity shading for enhanced perception of volumetric data. In *IEEE Visualization*, pp. 355–362.

Stewart, A. and M. Langer (1997). Towards accurate recovery of shape from shading under diffuse lighting. *IEEE Transactions on Pattern Analysis and Machine Intelligence 19*(9), 1020–1025.

Thelin, P. and R. Pike (1991). Landforms of the conterminous united states — a digital shaded–relief portrayal. Technical Report I–2206, US Geological Survey Miscellaneous Investigations Series Map (map and accompanying text).

Watt, A. (1999). *3D Computer Graphics*. Reading, MA: Addison–Wesley.

Weibel, R. and M. Heller (1991). *Digital Terrain Modelling*, Volume 1, pp. 269–297. New York: John Wiley & Sons.

Yokoyama, Ryuzo, Shirasawa, Michio, and R. Pike (2002). Visualizing topography by openness: A new application of image processing to digital elevation models. *Photogrammetric Engineering and Remote Sensing 68*(3), 257–265.

Zhou, Q. (1992). Relief shading using digital elevation models. *Computers and Geosciences 18*(8), 1035–1045.